Optical planar waveguides in Yb^{3+}-doped phosphate glasses produced by He^{+} ion implantation*

Liu Chun-Xiao(刘春晓)[a)b)], Li Wei-Nan(李玮楠)[a)], Wei Wei(韦 玮)[a)c)†], and Peng Bo(彭 波)[a)c)‡]

[a)] *State Key Laboratory of Transient Optics and Photonics, Xi'an Institute of Optics and Precision Mechanics, Chinese Academy of Sciences, Xi'an* 710119, *China*

[b)] *School of Electronic and Information Engineering, Hefei Normal University, Hefei* 230601, *China*

[c)] *Key Laboratory for Organic Electronics & Information Displays and Institute of Advanced Materials, Nanjing University of Posts & Telecommunications, Nanjing* 210046, *China*

(Received 8 September 2011; revised manuscript received 8 October 2011)

Optical planar waveguides in Yb^{3+}-doped phosphate glasses are fabricated by implanting triple-energy helium ions. The guiding modes and the near-field intensity distribution are measured by using the prism-coupling method and the end-face coupling setup with a He–Ne laser at 633 nm The intensity calculation method (ICM) is used to reconstruct the refractive index profile of the waveguide. The absorption and the fluorescence investigations reveal that the glass bulk features are well preserved in the active volumes of the waveguides, suggesting the fabricated structures for possible applications as waveguide lasers.

Keywords: waveguide, ion implantation, laser materials, photoluminescence

PACS: 42.79.Gn, 61.80.Jh, 61.43.Fs **DOI:** 10.1088/1674-1056/21/7/074211

1. Introduction

In the latest decade, Yb^{3+}-doped phosphate glasses have received much attention owing to their intriguing properties and potential applications. The Yb^{3+}-doped phosphate glasses exhibit high emission cross-sections, broad absorption, emission bands, and long fluorescence lifetime (1–2 ms), making them particularly attractive for generating ultrashort pulses and tunable laser sources. In addition, since there are only two manifolds in the Yb^{3+} energy level scheme (the $^2F_{7/2}$ ground state and $^2F_{5/2}$ excitation state), it is commonly believed that upconversion, excited state absorption, and concentration quenching have no effect on it. In the light of these merits, the Yb^{3+}-doped phosphate glass has the potential value to be used as a waveguide laser.[1−5]

The optical waveguide is one of the basic components in integrated optics and optoelectronics. The compact confinement of light propagating in waveguides of dimensions within order of microns results in very high optical intensities; consequently, some performances correlated to the bulks could be considerably enhanced in the waveguide structures.[6−9] For laser gain materials, the waveguide lasers possess lower pump thresholds and enhanced efficiencies, owing to the strongly reduced active volumes.[10] There are several techniques for fabricating waveguides in optical materials, which mainly include ion exchange,[11] femtosecond laser inscription,[12,13] and ion implantation.[14] Among these techniques, ion implantation can offer the most advantageous characteristics, that is, the wide applicability of materials. Moreover, it allows the accurate control of both dopant composition and penetration depth through the choice of the species and the energy of the ions.[15] Therefore, the combination of excellent laser performance of Yb^{3+}-doped phosphate glasses and effective waveguide technology of ion implantation is one promising solution to the realization of high-power integrated lasers with stable outputs. Furthermore, phosphate glasses are desirable materials for the fabrication of ion-implanted waveguides. Chen *et al.*[16] and Tan *et al.*[17] have fabricated planar and ridge

*Project supported by the National Natural Science Foundation of China (Grant Nos. 61077070, 10876009, and 51002181) and the One Hundred Talents Programs of the Chinese Academy of Sciences.

†Corresponding author. E-mail: weiwei@opt.ac.cn

‡Corresponding author. E-mail: bpeng@opt.ac.cn

© 2012 Chinese Physical Society and IOP Publishing Ltd

waveguides in Er^{3+}/Yb^{3+} co-doped phosphate glasses by using He ion implantation. In the present work, we report on the helium-implanted planar waveguides in Yb^{3+}-doped phosphate glasses, and study their guiding and luminescence performances.

2. Experiment

Yb^{3+}-doped phosphate glasses (doped with 1.5 mol% Yb_2O_3) were prepared under high temperature conditions by using the melt-quenching method. Each of them had a density of 2.97 g/cm^3 and a refractive index of 1.5324 (at 632.8 nm). The samples, each with a size of 10 mm×5 mm×2 mm, were optically polished and cleaned before the ion implantation. The planar waveguide was formed by keV He^+ ion implantation at room temperature at the Institute of Semiconductors, Chinese Academy of Sciences. In order to produce a broad barrier to avoid tunneling losses, a triple-implant process was performed on a single substrate of the Yb^{3+}-doped phosphate glass with energies of 450 keV, 500 keV, and 550 keV, and doses of 2×10^{16} ions/cm^2, 2×10^{16} ions/cm^2, 2×10^{16} ions/cm^2, respectively. After the ion implantation, the sample was annealed in a series of 60 min heat treatments at temperatures ranging from 260 °C to 410 °C in the air to further investigate the properties of the waveguide, and the specific annealing conditions are listed in Table 1.

Table 1. Annealing treatment conditions and the corresponding refractive indices for the samples implanted with helium ions.

Process	Annealing condition	Effective refractive index (TE_0)
S0	As-implanted	1.5165
S1	260 °C 60 min	1.5169
S2	S1+310 °C 60 min	1.5192
S3	S2+360 °C 60 min	1.5195
S4	S3+410 °C 60 min	1.5198

The planar waveguide in the Yb^{3+}-doped phosphate glass was characterized by using the well-known *m*-line technique, i.e., dark mode measurement (via Metricon 2010 Prism Coupler, USA) and the end-face coupling method at the wavelength of 632.8 nm. During the measurement of dark mode spectra, when the light was coupled into the waveguide, a lack of reflected light resulted in a dip, and the dip indicated the effective refractive index of the guided mode. In the latter case, a microscope objective lens (×25) focused the light beam into the waveguide to excite the guided modes, and another microscope objective lens (×25) collected the light from the output facet of the sample, which was imaged onto a CCD camera. The absorption spectra of the samples were recorded by using a spectrophotometer (Shimadzu, UV-3101PC) within the range of 850–1100 nm.

Confocal micro-luminescence experiments were performed by using a JY-T64000 laser-Raman spectrum system with an excitation wavelength of 532 nm at the Institute of Physics, Chinese Academy of Sciences. The micro-luminescence experiments were conducted by using a confocal microscope with a spatial resolution of 1 μm in combination with an XY motorized stage. The polarized light at 532 nm was focused onto the waveguide cross sections and the bulk (several microns away from the planar waveguide) by a 100× microscope objective. The emission band was back-collected by the same microscope objective and analyzed in a high-resolution spectrometer.

3. Results and discussion

Figure 1 shows the measured relative intensity of transverse electric (TE) polarized light at the wavelength of 632.8 nm reflected from the prism formed by the helium-implanted Yb^{3+}-doped phosphate glass planar waveguide after the S2 annealing treatment. As can be seen, the value of the observed mode is less than the corresponding refractive index of the substrate ($n_{sub} = 1.5324$), which implies that the planar waveguide is a typical barrier-confined structure.

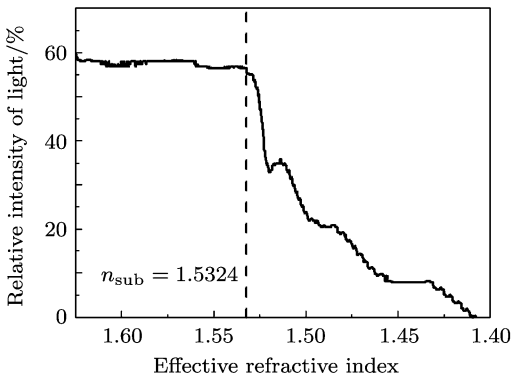


Fig. 1. Dark-mode spectrum of the TE mode for the He^+ ion-implanted waveguide of the Yb^{3+}-doped phosphate glass, where the dashed line represents the refractive index of the substrate.

The propagation modes of the planar waveguide are characterized by the end-face arrangement after the S4 annealing treatment. Figures 2(a) and

2(b) show the two-dimensional (2D) and the three-dimensional (3D) plots of the near-field intensity distribution (quasi-TE_0 mode) of the Yb^{3+}-doped phosphate glass planar waveguide, respectively. As can be seen, the light can be guided in a well confined way through the implanted index barrier. The propagation loss of the waveguide is also measured by using this end-face coupling system and estimated to be ~ 1.52 dB/cm.[18]

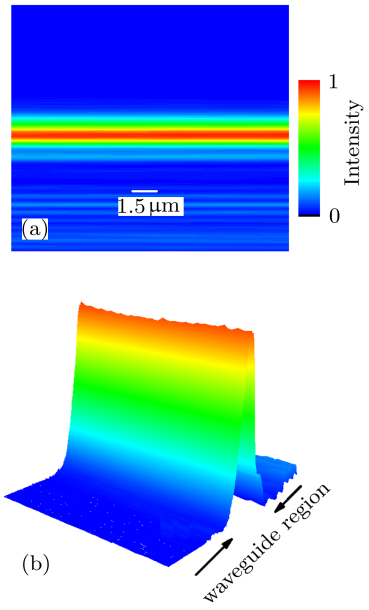


Fig. 2. (colour online) (a) 2D and (b) 3D plots of the near-field intensity distribution of the Yb^{3+}-doped phosphate glass planar waveguide.

For a better understanding of the mechanism of the planar waveguide formation in the Yb^{3+}-doped phosphate glass, we use the SRIM 2006 (stopping and range of ions in matter)[19] code to simulate the implantation process of 450 keV, 500 keV, and 550 keV He^+ ions into the Yb^{3+}-doped phosphate glass. Figure 3 shows the curves of electronic and nuclear energy losses of the incident He ions versus the penetration depth inside the glass. In most cases, although the electronic energy deposition is much larger than that of the nuclear one, the electronic excitations only create removable point defects, which have very slight effects on the refractive index of the substrate. On the other hand, the nuclear collisions can generate a buried layer at the end of the ion track, where decreases of both physical density and refractive index occur through the volume expansion induced by the nuclear damage, forming a waveguide structure between the barrier and the sample surface.[20–22]

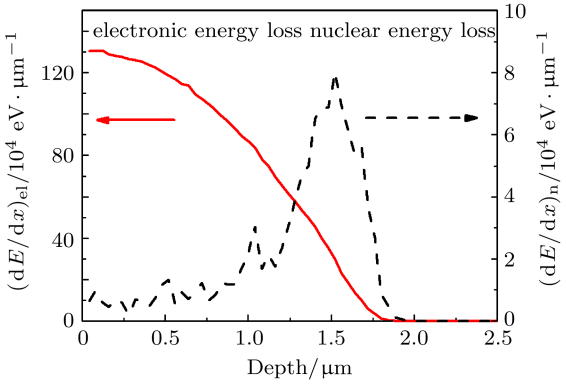


Fig. 3. (colour online) Distributions of electronic and nuclear energy losses of 450 keV, 500 keV, and 550 keV He ions implanted into the Yb^{3+}-doped phosphate glass simulated by SRIM 2006.

The refractive index distribution of a waveguide is very important for practical device design in real applications. In this work, we use the intensity calculation method (ICM)[23] to reconstruct the refractive index profile, which has been proved to be particularly successful for ion implanted waveguides of a single mode. As shown in Fig. 4, the refractive index in the waveguide region only slightly decreases after the implantation (~ 0.007), while in the barrier region, it reduces by ~ 0.05. In addition, the optical barrier is broadened to 0.2 μm after the triple-energy He^+ implantation, which may reduce the leakage effect of the modal field from the waveguide to the substrate. Therefore, the light can be confined between the barrier and the glass surface.

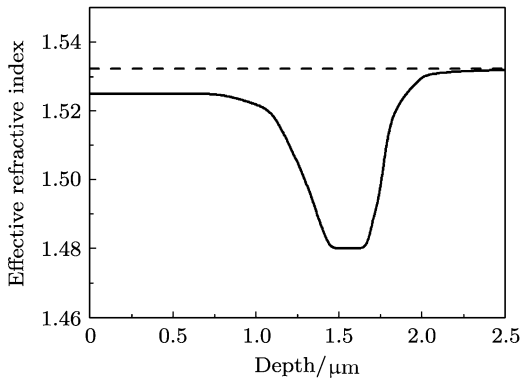


Fig. 4. Reconstructed refractive index profile of the Yb^{3+}-doped phosphate glass planar waveguide, where the dashed line represents the refractive index of the virgin glass.

In order to obtain a further understanding of the formation of the present waveguide formed by the 450 keV, 500 keV, and 550 keV helium implantation, we carry out continuous annealing treatments in atmosphere (Table 1).[24] After each annealing step, we

measure the dark mode spectrum of the waveguide and the corresponding effective refractive index of the TE_0 mode. The indices are given in Table 1 and Fig. 5. We can see that the effective refractive indices rise with the annealing treatment, which is due to the recovery of damages in the waveguide regions.

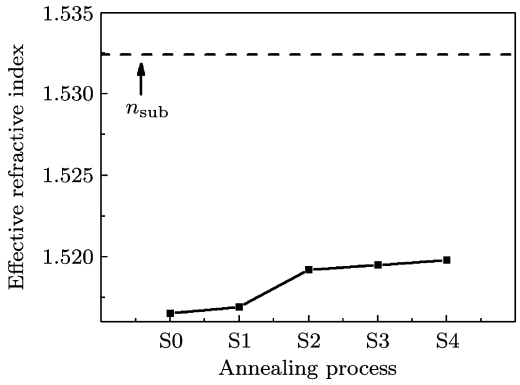


Fig. 5. Effective refractive indices of the TE_0 mode of the samples obtained after the annealing processes.

To investigate the effect of He implantation on the light absorption characteristics of the Yb^{3+}-doped phosphate glass, the absorption spectra are measured by using a Shimadzu UV-3101PC spectrophotometer. As depicted in Fig. 6, the spectrum of the Yb^{3+}-doped silicate waveguide is nearly the same as that of the substrate, including the shape, the peak position, and the intensity. Hence, there is almost no difference between the Yb^{3+}-doped phosphate substrate and the implanted sample, and we can say that the implantation process has almost no influence on the absorption properties.

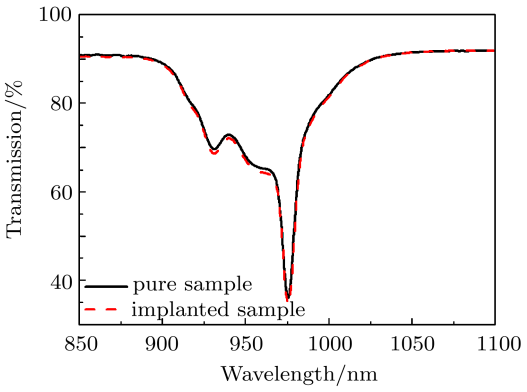


Fig. 6. (colour online) Absorption spectra of the ion-implanted and the pure Yb^{3+}-doped phosphate glasses.

For the practical applications involving optical gain, it is necessary to investigate the microphotoluminescence properties of the active waveguides.[25] Figure 7 shows the comparison between the room temperature micro-luminescence spectrum correlated to Yb^{3+} ions at $^2F_{5/2} \rightarrow ^2F_{7/2}$ transition obtained from the planar waveguide and that from the bulk obtained by a confocal fluorescence microscope (spectral range: 250–1000 nm). Unfortunately, because of the limitation of the spectrum range, we can only compare the emission spectra centred at 975 nm. As can be observed, the relevant spectrum from the planar waveguide is very similar in both shape and intensity to that from the bulk emission, indicating the absence of any defect-induced fluorescence quenching of Yb^{3+} ions in the waveguide. The data included in Fig. 7 shows that the outstanding luminescence features of Yb^{3+} ions are well preserved in the waveguide. This is an advantageous feature for laser applications, since it ensures low threshold laser oscillations.

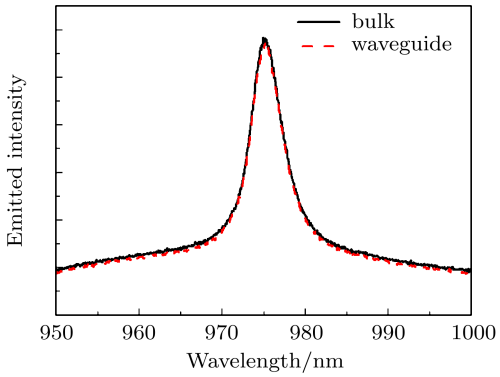


Fig. 7. (colour online) Room temperature micro-luminescence spectra correlated to Yb^{3+} ions at $^2F_{5/2} \rightarrow ^2F_{7/2}$ transition obtained from the planar waveguide and the bulk.

4. Summary

In this paper, we report on the fabrication of planar waveguides in Yb^{3+}-doped phosphate glasses by 450 keV, 500 keV, 550 keV helium implantation at the fluences of 2×10^{16} ions/cm^2, 2×10^{16} ions/cm^2, 2×10^{16} ions/cm^2, respectively. The waveguide properties are investigated by using prism-coupling and face-coupling methods. The annealing treatment results show that the planar waveguide has a high thermal stability. The microluminescence investigation shows that the waveguide exhibits a very similar emission spectrum to that of the bulk, which implies a potential application of the Yb^{3+}-doped phosphate glasses in waveguide lasers.

References

[1] Jiang C, Liu H, Zeng Q J, Tang X D and Gan F X 2000 *J. Phys. Chem. Sol.* **61** 1217

[2] Petrov V, Griebner U, Ehrt D and Seeber W 1997 *Opt. Lett.* **22** 408

[3] Boulon G 2008 *J. Alloys Compd.* **451** 1

[4] Veasey D L, Funk D S, Peters P M, Sanford N A, Obarski G E, Fontaine N, Young M, Peskin A P, Liu W C, Houde-Walter S N and Hayden J S 2000 *J. Non-Cryst. Solids* **263&264** 369

[5] Zhou W L, Zhang Q L, Gao J Y, Liu W P, Ding L H and Yin S T 2011 *Chin. Phys.* B **20** 016101

[6] Kip D 1998 *Appl. Phys.* B **67** 131

[7] Stegeman G I and Seaton C T 1985 *J. Appl. Phys.* **58** R57

[8] Wang X L, Chen F, Lu F, Fu G, Li S L, Wang K M, Zhang H J, Shen D Y, Ma H J and Nie R 2004 *Chin. Phys. Lett.* **21** 867

[9] Jiang Y, Wang K M, Chen F, Wang X L, Jia C L, Wang L, Shen D Y, Ma H J and Nie R 2006 *Chin. Phys. Lett.* **23** 922

[10] Mackenzie J I 2007 *IEEE J. Sel. Top. Quantum Electron.* **13** 626

[11] Shao G W and Jin G L 2009 *Chin. Phys.* B **18** 1096

[12] Valle G D, Osellame R, Chiodo N, Taccheo S, Cerullo G, Laporta P, Killi A, Morgner U, Lederer M and Kopf D 2005 *Opt. Express* **13** 5976

[13] Chan J W, Huser T R, Risbud S H, Hayden J S and Krol D M 2003 *Appl. Phys. Lett.* **82** 2371

[14] Berneschi S, Nunzi Contil G, Banyasz I, Watterich A, Khanh N Q, Fried M, Paszti F, Brenci M, Pelli S and Righini G C 2007 *Appl. Phys. Lett.* **90** 121136

[15] Chen F, Wang X L and Wang K M 2007 *Opt. Mater.* **29** 1523

[16] Chen F, Wang X L, Li X S, Hu L L, Lu Q M, Wang K M, Shi B R and Shen D Y 2002 *Appl. Surf. Sci.* **193** 92

[17] Tan Y, Chen F, Hu L L, Xing P F, Chen Y X, Wang X L and Wang K M 2007 *J. Phys.* D: *Appl. Phys.* **40** 6545

[18] Regener R and Sohler W 1985 *Appl. Phys.* B **36** 143

[19] Biesack J P 2011 *SRIM* http://www.srim.org

[20] Qin X F, Chen M, Wang X L, Liang Y and Zhang S M 2010 *Chin. Phys.* B **19** 113403

[21] Chen F 2009 *J. Appl. Phys.* **106** 081101

[22] Domenech M, Vázquez G V, Flores-Romero E, Cantelar E and Lifante G 2005 *Appl. Phys. Lett.* **86** 151108

[23] Liu X Z, Lu F, Chen F, Tan Y, Zhang R, Liu H, Wang L and Wang L L 2008 *Opt. Commun.* **281** 1529

[24] Tan N and Zhang Q Y 2006 *Chin. Phys.* **15** 2165

[25] Silva W F, Jacinto C, Benayas A, de Aldana J R, Torchia G A, Chen F, Tan Y and Jaque D 2010 *Opt. Lett.* **35** 916